

Boundary effect on the plasticity and stress of lithiated silicon: First-principles calculations

H. Y. Lv,^{1,2} H. Jiang,^{2,a)} H. J. Liu,^{1,b)} and J. Shi¹

¹Key Laboratory of Artificial Micro- and Nano-Structures of Ministry of Education and School of Physics and Technology, Wuhan University, Wuhan 430072, China

²School for Engineering of Matter, Transport and Energy, Arizona State University, Tempe, Arizona 85287, USA

(Received 15 August 2012; accepted 12 October 2012; published online 21 November 2012)

Silicon anode experiences large volumetric change ($\sim 400\%$) during lithiation in lithium ion batteries, which induces fracture and plasticity. In this paper, the boundary effect of silicon nanofilms on the structural evolution, plasticity, stress, and strain during lithiation is studied by first-principles calculations. It is found that rigid boundary induces compression stress and structural disruption during lithiation, as well as voids and plastic deformation during delithiation. In contrast, free boundary allows silicon to expand freely and release the stress during lithiation. Moreover, the volume expansion of the lithiated Si is totally recoverable during delithiation and thus the deformation is entirely elastic. © 2012 American Institute of Physics.

[<http://dx.doi.org/10.1063/1.4765689>]

Silicon (Si) is considered to be one of the most promising anode materials in lithium (Li) ion batteries due to its highest known specific capacity, 4200 mAh/g,¹ which is one order of magnitude higher than that of the present anode material, graphite (372 mAh/g). However, upon insertion and extraction of Li during charge and discharge cycling, Si experiences large volume expansion (up to $\sim 400\%$),² which will pulverize the electrodes.³ This has been one of the main bottlenecks in the commercial use of Si in Li-ion batteries. In recent years, many efforts have been made to minimize the pulverization and the capacity loss. In particular, Si nanostructures such as Si nanowires,^{4–6} nanotubes,^{7–9} and nanofilms^{10–12} have been studied to improve the performance by various stress relaxation mechanisms. In parallel, there have been some efforts to understand the origin of fracture in lithiated Si. For example, Sethuraman *et al.*¹³ used optical methods to *in-situ* measure the stress evolution in lithiated/delithiated Si film and a novel feature, plasticity, has been observed in this classic material which is usually considered to be brittle. Zhao *et al.*¹⁴ conducted first-principles calculations to study the stress/strain relations of various Si/Li alloys and plasticity was found to present when Li composition is high. In a recent work,¹² it was found that Si nanofilms on soft substrate can significantly improve the cyclic retention, which seems to suggest that the constraint on Si anode plays an important role. In this paper, the boundary effects on the lithiation-induced structural evolution, plasticity, stress, and strain of Si nanofilms are studied by using first-principles pseudopotential method. Both fixed and free boundaries are examined. It should be pointed out that the central theme of this work is the effect of boundary condition on plasticity of lithiated Si but not the kinetic process (e.g., diffusion). Therefore, the following study is static rather than dynamic.

Our calculations are performed via a plane-wave pseudopotential formulation^{15–17} within the framework of density functional theory (DFT). The code is implemented in the Vienna *ab initio* simulation package (VASP). The electron-ion interaction is modeled using the projector-augmented wave (PAW) technique.^{18,19} The exchange-correlation energy is in the form of PW91²⁰ and the cutoff energy for the plane wave expansion is set to be 800 eV. All the structures are fully relaxed until the magnitude of the forces acting on all the atoms becomes less than 0.04 eV/Å.

A unit cell including 34 Si atoms is employed to model a Si (001) nanofilm with thickness of ~ 23.5 Å. The Si atoms on the top and bottom surfaces are passivated by hydrogen (H) atoms. A vacuum layer of 15 Å is applied to separate the repeated slabs, which is large enough to avoid any artificial interaction between periodic images. Figure 1 shows the side views of Si nanofilm from two different directions. For the fully relaxed structure, the lattice constant a is calculated to be 5.52 Å, which is very close to the experimental value of 5.43 Å²¹ for the conventional cubic cell of bulk Si.

As mentioned before, we consider two types of boundary condition, namely, the completely rigid and free boundaries. The rigid boundary is used to model the case that Si nanofilm anodes are on rigid current collectors,¹⁰ in which the Si nanofilms can only deform along the out-of-plane direction but not the in-plane direction. This boundary condition is implemented by freezing the H atoms on the bottom and the associated Si atoms. The free boundary represents a scenario that Si nanofilm anodes are on a very soft substrate,¹² in which the Si nanofilms can deform freely along all the three directions and the unit cell is thus relaxed.

To model the lithiation process when the Si nanofilm is charged, Li atoms diffuse into the Si nanofilm and tend to occupy the tetrahedral (Td) positions, which are believed to be energetically most favorable.²² An assumption of an extremely low charge rate is used in the calculations and thus the Li atoms have enough time to diffuse into those

^{a)}Email: hanqing.jiang@asu.edu.

^{b)}Email: phlhj@whu.edu.cn.

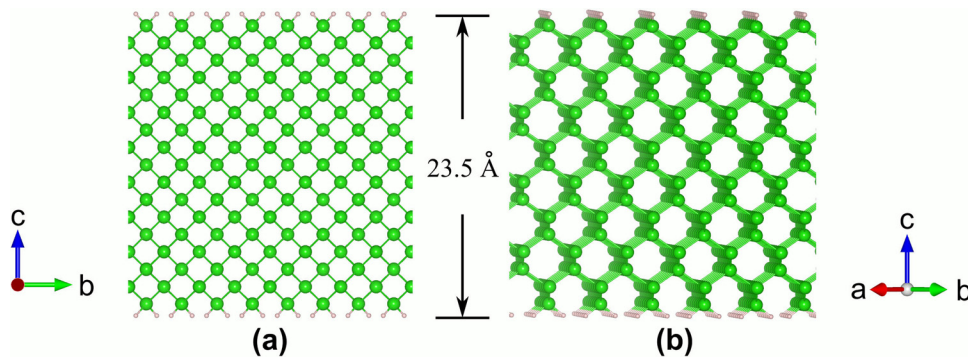


FIG. 1. Ball-and-stick model of pristine Si (001) nanofilm viewed from two different directions. The green and pink balls represent Si and H atoms, respectively. The width of the nanofilm is 23.5 Å.

energetically most favorable sites (i.e., Td positions). This situation can also be imagined as the formation of Si/Li alloy followed by annealing. It is also reported that the Li atoms tend to separate each other to form a homogeneous doping distribution when the concentration is low.²³ Considering all these factors, we assume that in initial structures Li atoms are homogeneously distributed at each concentration and at the same time they are separated as far as possible from each other. Upon structural relaxations, the Li atoms may distribute inhomogeneously as to be shown in the following, particularly for relatively higher Li concentration.

We begin with the rigid boundary condition. As Li diffuses into the Si nanofilm, different phases of Li_xSi are formed, where x represents the ratio between the number of Li atoms to that of Si atoms in the unit cell. It should be noticed that x is related to but different from the conventional concentration as the maximum value of x is 4.4 based on the $\text{Li}_{22}\text{Si}_5$ structure.¹ However, to make the description concise, we still use x as the Li concentration. Figure 2 shows the structural evolution of Si nanofilm with rigid boundary upon lithiation, where six different Si/Li phases are investigated. The following criterion is used to determine the Si-Si bond breaking and reformation: two Si atoms are bonded if the deformation of the bond length is within 20% compared to that in bulk Si, which corresponds to a largest distance of 2.87 Å; otherwise, the Si-Si bonds are broken.¹⁴ The first impression from Fig. 2 is that with the increase of Li concentration (i.e., x varies from 0.06 to 1.00), the nanofilm expands in the vertical direction and the in-plane directions remain unchanged, which indicates that the rigid boundary has been realized. The second impression from Fig. 2 is the Si-Si bond breaking and reformation. As shown

in Figs. 2(a)–2(d), for smaller x varying from 0.06 to 0.29, the Si nanofilm maintains good crystal structure which is almost the same as pristine Si nanofilm. However, when x increases to 0.53, as shown in Fig. 2(e), some Si-Si bonds are broken and at the same time new Si-Si bonds are formed. When x increases further from 0.53 to 1, we see from Fig. 2(f) that the newly formed bonds are broken and at the same time, some originally connected bonds are also broken. Due to the breaking and reformation of Si-Si bonds, the Si nanofilms become partially disordered, as circled by the purple lines in Figs. 2(e) and 2(f). This structural change may result in cracking of Si anodes. It is also noticed that Li atoms are inhomogeneously distributed for relatively high Li concentration (e.g., Figs. 2(e) and 2(f)) even uniform distribution is used in their initial structures.

The stress in the lateral direction can be obtained from the derivative of the free energy in our calculations. Figure 3(a) shows the evolution of the lateral stress as a function of Li concentration x . The first data point corresponds to the pristine Si nanofilm and the following six data points correspond to the six Si/Li phases shown in Fig. 2. The black solid line is for lithiation while the red dashed lines indicate delithiation. As the Si nanofilm is charged, the compressive stress is developed as a result of the rigid boundary in the lateral directions. When x is relatively small ($x \leq 0.15$), the absolute value of the compressive stress increases as x increases and it reaches the local maximum at $x = 0.15$. For these phases, if Li is removed, the lateral stresses retract to zero as shown by the red dashed lines. This implies that for low Li concentration, the lithiated Si is still under the elastic deformation, which is consistent with the observations that the crystal structures remain and there is no bond breaking and

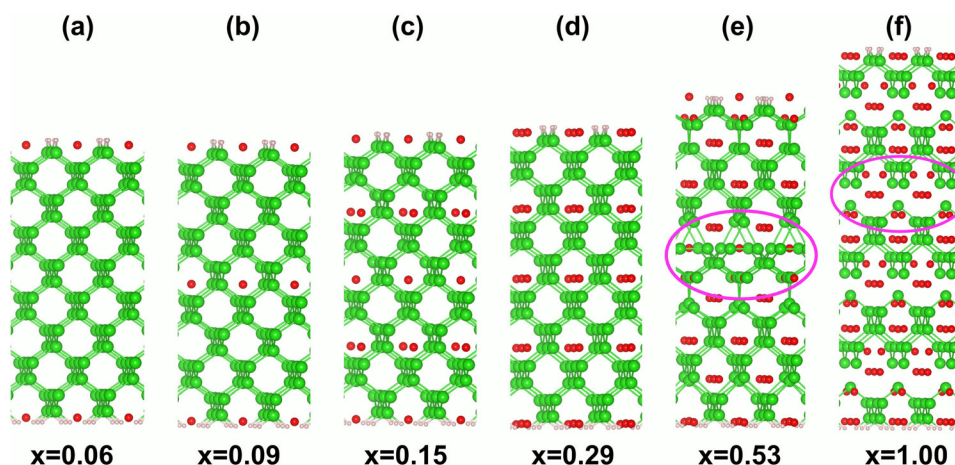


FIG. 2. Evolution of the Si nanofilm structure upon lithiation for rigid substrate: (a), (b), (c), (d), (e), and (f) with Li concentration $x=0.06$, 0.09, 0.15, 0.29, 0.53, and 1.00, respectively. The red balls represent Li atoms.

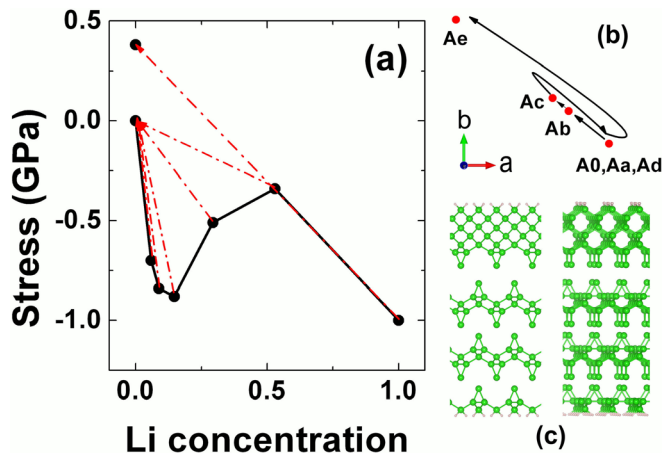


FIG. 3. (a) Evolution of the stress in Si nanofilm as a function of Li concentration x for rigid substrate. (b) Top view of the trajectory of a Si atom inside the Si nanofilm for different Li concentrations. Position A_0 corresponds to the pristine film, while A_a , A_b , A_c , A_d , and A_e correspond to Li concentration $x = 0.06, 0.09, 0.15, 0.29$, and 0.53 , respectively. (c) Structures of delithiated Si nanofilm for $x = 1.0$ viewed from two different directions shown in Fig. 1.

reformation (Figs. 2(a)–2(c)). Further increase of x leads to less compressive lateral stress and the lithiated Si seems to be softened. The exact reason for softening is not very clear but our speculation is that it may be caused by nonsymmetrical motions of some internal Si atoms as Li atoms are inserted (Figs. 2(c) and 2(d)). Fig. 3(b) illustrates the trajectory of a particular Si atom from its initial position (marked as A_0), to position A_c for Fig. 2(c) and A_e for Fig. 2(e). The change of these locations is due to the way that the Li atoms are inserted. It is somewhat similar to instability or bifurcation and worth further study. More interestingly, even at the softening stage, the delithiated Si nanofilms can be relaxed to the vanishing stress state, as shown by the red dashed lines shown in Fig. 3(a). This suggests that the softened lithiated Si is still under the elastic deformation, which is very different from the classical metallic materials where the softening usually means plastic deformation. As Li concentration continuously increasing, the compressive stress increases again and it reaches 1.0 GPa at $x = 1.0$. At this stage the delithiation cannot recover to the vanishing stress state, which means that

the structure destruction is permanent and the plastic deformation occurs. Therefore, under the confined boundary conditions that is the common case in almost all experiments, the nonlinearity between Si stress and Li concentration does not necessarily indicate plasticity but the structural recoverability during delithiation is a measure of plasticity. As shown in Fig. 3(c), the delithiated Si shows many broken and reformed Si-Si bonds, which can be considered as cracks and voids in the Si nanofilms. It should be mentioned that we have also considered the delithiation layer by layer, i.e., removing Li atoms from the lithiated Si from the top to bottom. Our calculations indicate that the structure destruction develops from the top to bottom of Si nanofilm. Indeed, the development and evolution of cracks and voids were previously identified in experiments. Huang *et al.*²⁴ first reported the *in situ* observation of a reaction front in SnO₂ nanowire. This reaction front contains mobile dislocations, which indicate large in-plane misfit stress and the amorphization of the nanowire. The phenomenon is observed in Si nanowire as well.²⁵

We now move to the discussions with free boundary conditions in the lateral direction. In this case, the Si nanofilm is fully relaxed in all directions and the stress is totally released. We also assume that Li atoms distribute uniformly in the Si nanofilms for the initial structures. Figures 4(a)–4(f) show the structural evolution of the Si nanofilm upon lithiation. Unlike the case where the Si nanofilm is fixed in the lateral directions, we now find that the lithiated Si nanofilms retain the crystal structure even for relatively higher Li concentration ($x = 1.0$). This is reasonable since the free boundary conditions allow the lithiated Si to expand in the lateral directions and release the compressive stress. Fig. 4(g) plots the strain along the lateral direction of the Si nanofilm as a function of Li concentration x . As the stress is released in the lateral direction, the strain is actually the eigenstrain due to lithiation. In other words, this curve gives a lithiation eigenstrain as a function of Li composition in the Si/Li alloy, which can be used to describe the compositional expansion during lithiation in many continuum level simulations.^{26,27} The nonlinear behavior shown in Fig. 4(g) suggests that more thorough studies are needed to understand how Si expands during lithiation. For delithiation, the strain retrieves to zero as the

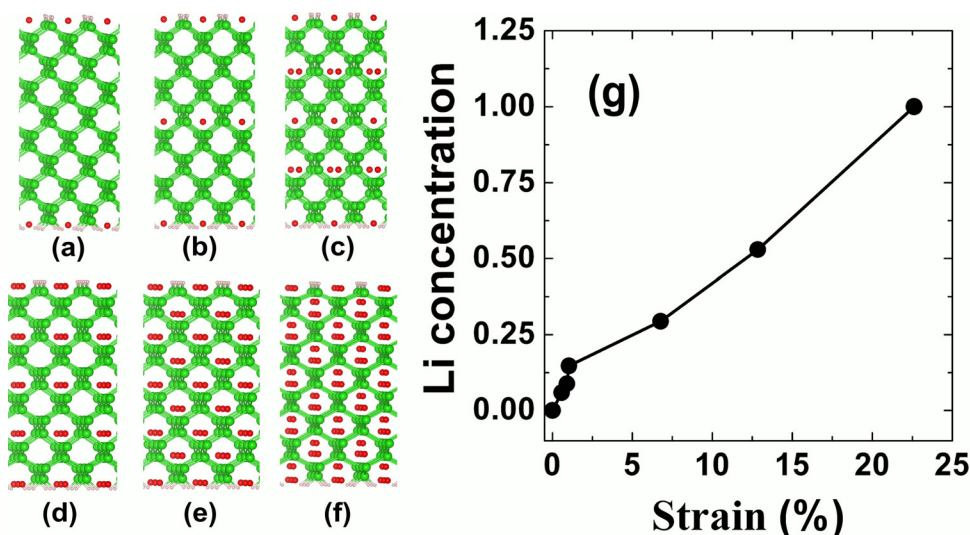


FIG. 4. Evolution of the Si nanofilm structure upon lithiation for free substrate: (a), (b), (c), (d), (e), and (f) with Li concentration $x = 0.06, 0.09, 0.15, 0.29, 0.53$, and 1.00 , respectively. The strain in Si nanofilm as a function of x is plotted in (g).

structure is not distorted (Figs. 4(a)–4(f)), so the lithiation is an elastic deformation for Si nanofilms with free boundary conditions. This result seems to suggest a means to keep the lithiation process elastic by removing the constraints.

In conclusion, we have investigated the effect of boundary conditions on the lithiated Si nanofilms using first-principles calculations. The evolution of structure, stress, and strain as a function of Li composition are discussed. The rigid boundary induces compression stress and leads to structural disruption. The delithiation then introduces voids and the plastic deformation presents, which is unfavorable for the retention of Si anodes in Li-ion batteries. On the other hand, the free boundary allows the lithiated Si to expand freely and release the stress. The structure of the lithiated Si is intact and the expansion is totally recoverable. The deformation is entirely elastic, which is highly desirable in the Li-ion batteries applications using Si as anodes. We must admit that our calculations are only for ideal situations, i.e., completely rigid or free substrates and extremely slow charge rate. However, our results still qualitatively explain the related experiments. For example, when the substrate becomes softer, the stress relaxation can be realized and better retention is expected. In fact, it has been reported that soft substrate can release the stress by buckling the Si nanofilms during charge/discharge cycles, which in turn provides better cyclic retention for Si anodes.¹²

H.Y.L., H.J.L., and J.S. acknowledge financial support from the China Scholarship Council and the NSFC 51172167. H.J. acknowledges the support from NSF CMMI-1067947 and CMMI-1162619. We also appreciate the Fulton High Performance Computing at Arizona State University to support our simulations.

¹B. A. Boukamp, G. C. Lesh, and R. A. Huggins, *J. Electrochem. Soc.* **128**, 725 (1981).

²U. Kasavajjula, C. S. Wang, and A. J. Appleby, *J. Power Sources* **163**, 1003 (2007).

³R. A. Huggins and W. D. Nix, *Ionics* **6**, 57 (2000).

⁴C. K. Chan, H. L. Peng, G. Liu, K. McIlwrath, X. F. Zhang, R. A. Huggins, and Y. Cui, *Nat. Nanotechnol.* **3**, 31 (2008).

⁵K. Kang, H.-S. Lee, D.-W. Han, G.-S. Kim, D. Lee, G. Lee, Y.-M. Kang, and M.-H. Jo, *Appl. Phys. Lett.* **96**, 053110 (2010).

⁶J. W. Choi, J. McDonough, S. Jeong, J. S. Yoo, C. K. Chan, and Y. Cui, *Nano Lett.* **10**, 1409 (2010).

⁷M.-H. Park, M. G. Kim, J. Joo, K. Kim, J. Kim, S. Ahn, Y. Cui, and J. Cho, *Nano Lett.* **9**, 3844 (2009).

⁸W. Wang and P. N. Kumta, *ACS Nano* **4**, 2233 (2010).

⁹T. Song, J. L. Xia, J.-H. Lee, D. H. Lee, M.-S. Kwon, J.-M. Choi, J. Wu, S. K. Doo, H. Chang, W. I. Park, D. S. Zang, H. Kim, Y. G. Huang, K.-C. Hwang, J. A. Rogers, and U. Paik, *Nano Lett.* **10**, 1710 (2010).

¹⁰T. Takamura, S. Ohara, M. Uehara, J. Suzuki, and K. Sekine, *J. Power Sources* **129**, 96 (2004).

¹¹S. Ohara, J. Suzuki, K. Sekine, and T. Takamura, *J. Power Sources* **136**, 303 (2004).

¹²C. J. Yu, X. Li, T. Ma, J. P. Rong, R. J. Zhang, J. Shaffer, Y. H. An, Q. Liu, B. Q. Wei, and H. Q. Jiang, *Adv. Energy Mater.* **2**, 68 (2012).

¹³V. A. Sethuraman, M. J. Chon, M. Shimshak, V. Srinivasan, and P. R. Guduru, *J. Power Sources* **195**, 5062 (2010).

¹⁴K. J. Zhao, W. L. Wang, J. Gregoire, M. Pharr, Z. G. Suo, J. J. Vlassak, and E. Kaxiras, *Nano Lett.* **11**, 2962 (2011).

¹⁵G. Kresse and J. Hafner, *Phys. Rev. B* **47**, 558 (1993).

¹⁶G. Kresse and J. Hafner, *Phys. Rev. B* **49**, 14251 (1994).

¹⁷G. Kresse and J. Furthmüller, *Comput. Mater. Sci.* **6**, 15 (1996).

¹⁸P. E. Blöchl, *Phys. Rev. B* **50**, 17953 (1994).

¹⁹G. Kresse and D. Joubert, *Phys. Rev. B* **59**, 1758 (1999).

²⁰J. P. Perdew and Y. Wang, *Phys. Rev. B* **45**, 13244 (1992).

²¹P. Becker, P. Seyfried, and H. Siebert, *Z. Phys. B* **48**, 17 (1982).

²²T.-L. Chan and J. R. Chelikowsky, *Nano Lett.* **10**, 821 (2010).

²³W. H. Wan, Q. F. Zhang, Y. Cui, and E. G. Wang, *J. Phys.: Condens. Matter* **22**, 415501 (2010).

²⁴J. Y. Huang, L. Zhong, C. M. Wang, J. P. Sullivan, W. Xu, L. Q. Zhang, S. X. Mao, N. S. Hudak, X. H. Liu, A. Subramanian, H. Fan, L. Qi, A. Kushima, and J. Li, *Science* **330**, 1515 (2010).

²⁵X. H. Liu, H. Zheng, L. Zhong, S. Huang, K. Karki, L. Q. Zhang, Y. Liu, A. Kushima, W. T. Liang, J. W. Wang, J.-H. Cho, E. Epstein, S. A. Dayeh, S. T. Picraux, T. Zhu, J. Li, J. P. Sullivan, J. Cumings, C. Wang, S. X. Mao, Z. Z. Ye, S. Zhang, and J. Y. Huang, *Nano Lett.* **11**, 3312 (2011).

²⁶Y. An and H. Jiang, "A finite element simulation on transient large deformation and mass diffusion in electrodes for lithium ion batteries" (submitted).

²⁷N. Swaminathan, J. Qu, and Y. Sun, *Philos. Mag.* **87**, 1705 (2007).